

This is the accepted manuscript made available via CHORUS. The article has been published as:

Bose-Einstein condensates in a ring-shaped trap with a nonlinear double-well potential

Xiang-Fa Zhou, Shao-Liang Zhang, Zheng-Wei Zhou, Boris A. Malomed, and Han Pu
Phys. Rev. A **85**, 023603 — Published 3 February 2012

DOI: [10.1103/PhysRevA.85.023603](https://doi.org/10.1103/PhysRevA.85.023603)

Bose-Einstein condensates in a ring-shaped trap with a nonlinear double-well potential

Xiang-Fa Zhou¹, Shao-Liang Zhang¹, Zheng-Wei Zhou¹, Boris A. Malomed², and Han Pu³

¹*Key Laboratory of Quantum Information, University of Science and Technology of China, Hefei, Anhui 230026, P. R. China*

²*Department of Physical Electronics, School of Electrical Engineering, Faculty of Engineering, Tel Aviv University, Tel Aviv 69978, Israel*

³*Department of Physics and Astronomy, and Rice Quantum Institute, Rice University, Houston, Texas 77251-1892, USA*

We develop the mean-field theory for Bose-Einstein condensates (BECs) in a one-dimensional ring with two types of nonlinear double-well potentials, based on a pair of delta-functions or Gaussian of a finite width, placed at diametrically opposite points. Analyzing the ground states (GSs) in these cases, we find a qualitative difference between them: with the Gaussian profile, the GS always undergoes the phase transition from the symmetric shape to an asymmetric one at a critical value of the norm. On the contrary, the symmetry-breaking transition does not happen with the δ -functional profile of the nonlinearity, the GS always remaining symmetric. In addition, the numerical analysis for the Gaussian profile demonstrates that the type of the symmetry-breaking transition depends on the width of the nonlinear-potential well.

PACS numbers: 03.75.Lm, 05.45.Yv

I. INTRODUCTION

Hohenberg has proved that Bose-Einstein condensation (BEC) does not occur in an interacting infinitely extended uniform bosonic system for low dimensional systems, even at the zero temperature, since long-wavelength phase fluctuations destroy the off-diagonal long-range order [1]. However, this is not true in spatially confined finite systems [2]. In line with the latter fact, stable effectively one-dimensional (1D) BEC and matter-wave solitons in it have been observed experimentally in ultracold gases of ⁷Li [3, 4] and ⁸⁵Rb [5] atoms. More recently, BEC on a ring has been experimentally demonstrated by quite a few groups [6]. These achievements make it possible to experimentally realize spatially confined low-dimensional condensates subject to periodic boundary conditions. Further, making use of the fact that both the magnitude and sign of the parameter governing the intrinsic nonlinearity of the condensate — the scattering length of the atomic collisions — can be tuned, using externally applied magnetic [7] or optical [8, 9] fields via the Feshbach resonance technique [10], a method to generate periodically modulated patterns of the scattering length (*nonlinear lattices*) and other effective nonlinear potentials (alias *pseudopotentials*) has been elaborated and applied to solitons in various settings, see original works [11] and recent review [14], and to bound states of two atoms, at the most fundamental level [15]. Combining these ingredients, in this work we aim to consider the dynamics of BEC in the ring-shaped trap with an intrinsic nonlinear potential.

Many theoretical results have been reported for bosons confined in a 1D finite system with periodic boundary conditions [16, 17], and in the ring-shaped traps [18, 19]. In particular, within the mean-field (MF) theory, these systems feature a quantum phase transition (QPT) between a uniform condensate and a bright soliton state

when the strength of attractive interactions approaches a critical value. Roughly speaking, the QPT is caused by the competition between the quantum pressure and self-attraction. A similar QPT takes place in the system of bosons confined in a 1D nonlinear ring-shaped lattice [12, 20]. In such a system, the atomic scattering length is periodically modulated between negative and positive values as $U = U_0 \sin(d\theta)$, where d is the modulation period and θ is the azimuthal angle along the ring. When the depth of the periodic modulation U_0 exceeds a certain critical value, the MF ground state (GS) undergoes a QPT from a spatially periodic state into a soliton-like one. Reference [12] shows that the nature of the QPT is also sensitive to the modulation period d . In particular, the MF symmetry-breaking phase transition is of the second kind when the modulation period is 2, and of first kind when the period is larger than 2.

Additionally, the above-mentioned double-well nonlinear in a ring geometry can also be considered in dipolar BECs. For instance, an effective ring-shaped two-period modulated nonlinear potential is achieved when the alignment of the atomic dipoles is perpendicular to the symmetry axis of ring traps, where symmetry breaking phenomena has also been predicted under MF level [21]. Therefore, this can be viewed as another ideal experimental platform to testify the model we discussed here.

In this paper we investigate MF states of the BEC in a ring-shaped trap with two types of the intrinsic nonlinear double-well potentials, δ -functional and Gaussian with a finite width. We find that the δ -type of the nonlinear potential leads to a degenerate behavior, which cannot be approximated by the Gaussian-type potentials with any finite width. The GS is always symmetric within a small regime of the norm. We also find that, if the pair of Gaussians is used, the system shows a QPT from a symmetric GS to an asymmetric one as we increase the

norm. The width of the Gaussian is a key parameter to determine the type of the QPT.

This paper is organized as follows. The model's Hamiltonian is introduced in section II. Section III presents analytical solutions for the δ -functional nonlinearity. In section IV, we numerically investigate the GS and QPT for the Gaussian profile. Discussions and conclusions are presented in sections V and Sec. VI, respectively.

II. THE HAMILTONIAN

The system considered here is similar to the one studied in Ref. [12, 18, 20]. N bosons are confined in a toroid of radius R and cross-section area S . The normalized Hamiltonian for such a system can be written as

$$H = \int_0^{2\pi} d\theta \left[-\psi^\dagger(\theta) \frac{\partial^2}{\partial \theta^2} \psi(\theta) + \frac{U}{2} \psi^\dagger(\theta) \psi^\dagger(\theta) \psi(\theta) \psi(\theta) \right], \quad (1)$$

where θ is the azimuthal angle around the toroid, defined so that it takes values $-\pi/2 < \theta \leq 3\pi/2$. The two terms in H represent the kinetic and potential energies, which are measured in units of $\hbar^2/(2mR^2)$, where m is the bosonic mass, while the dimensionless interaction strength is $U = 8\pi a_s R/S$, with the (tunable) s -wave scattering length a_s . A related problem in an open (infinite) 1D system was studied in Refs. [13, 22].

We consider a situation where the scattering length, hence the interaction strength U too, are modulated along the toroid, with two types of the modulation. First, we consider a pair of δ -functions located at diametrically opposite points,

$$U(\theta) = -[\delta(\theta - \pi/2) + \delta(\theta - 3\pi/2)]. \quad (2)$$

Second, we consider a smooth modulation, with the δ -functions replaced by Gaussians of a finite width a in terms of azimuthal coordinate

$$U(\theta) = -\frac{1}{a\sqrt{\pi}} \left[\exp\left(-\frac{(\theta - \pi/2)^2}{a^2}\right) + \exp\left(-\frac{(\theta - 3\pi/2)^2}{a^2}\right) \right]. \quad (3)$$

In the limit $a \rightarrow 0$, the Gaussians reduce to the δ -functions.

The corresponding Gross-Pitaevskii (GP) equation can be derived from Hamiltonian (1) as

$$i \frac{\partial}{\partial t} \psi(\theta, t) = -\frac{1}{2} \frac{\partial^2}{\partial \theta^2} \psi(\theta, t) + U(\theta) |\psi|^2 \psi(\theta, t). \quad (4)$$

Setting $\psi(\theta, t) = \phi(\theta) e^{-i\mu t}$, we arrive at the stationary version of the GP equation with chemical potential μ ,

$$\mu \phi = -\frac{1}{2} \frac{\partial^2}{\partial \theta^2} \phi + U(\theta) |\phi|^2 \phi, \quad (5)$$

Finally, the norm of the wave function is defined as

$$N = \int d\theta |\phi(\theta)|^2. \quad (6)$$

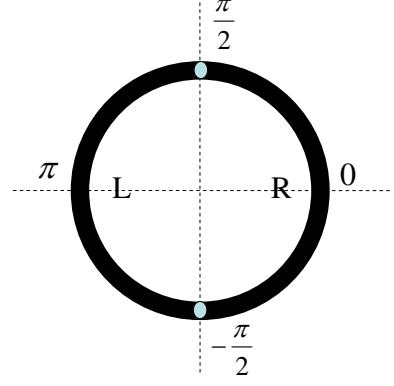


FIG. 1: A sketch of the system. The two gray dots represent the positions of the nonlinear potential, around which the interaction strength is modulated. Values of azimuthal coordinate, θ , are indicated as defined in the text.

III. THE ANALYTICAL SOLUTION FOR THE DELTA-FUNCTIONS

We first consider the δ -nonlinearity with the interaction strength given by Eq. (2). It is convenient to divide the toroid into two segments, $(-\pi/2, \pi/2)$ and $(\pi/2, 3\pi/2)$, to be denoted “R” and “L”, respectively, see Fig. 1. Off points $\theta = \pi/2$ and $3\pi/2$, Eq. (4) is linear, hence its solution can be written as

$$\phi_R(\theta) = A_R \cos(\sqrt{2\mu}\theta) + B_R \sin(\sqrt{2\mu}\theta), \quad (7a)$$

$$\phi_L(\theta) = A_L \cos(\sqrt{2\mu}(\pi - \theta)) + B_L \sin(\sqrt{2\mu}(\pi - \theta)), \quad (7b)$$

for $\mu > 0$. For $\mu < 0$, the solution is

$$\phi_R(\theta) = A_R \cosh(\sqrt{2|\mu|}\theta) + B_R \sinh(\sqrt{2|\mu|}\theta), \quad (8a)$$

$$\phi_L(\theta) = A_L \cosh(\sqrt{2|\mu|}(\pi - \theta)) + B_L \sinh(\sqrt{2|\mu|}(\pi - \theta)). \quad (8b)$$

Here we concentrate on the case of $\mu < 0$ case, a similar analysis being possible for $\mu > 0$ too. The continuity condition for the wave function at the points $\theta = \pi/2$ and $3\pi/2$ requires

$$\phi_R(\pi/2) = \phi_L(\pi/2), \quad \phi_R(-\pi/2) = \phi_L(3\pi/2), \quad (9)$$

which impose the following restrictions on the coefficients $A_{L,R}$ and $B_{L,R}$ in expressions (8):

$$A_R \cosh(\alpha) \pm B_R \sinh(\alpha) = A_L \cosh(\alpha) \mp B_L \sinh(\alpha), \quad (10)$$

where $\alpha \equiv \sqrt{2|\mu|}\pi/2$. Therefore, one may only have $A_L = A_R \equiv A$ and $B_L = B_R \equiv B$.

On the other hand, integrating the GP equation in the vicinity of the two δ -functions, we arrive at the following jump conditions for the first derivative of the wave function:

$$\begin{aligned} \phi'_L(\pi/2) - \phi'_R(\pi/2) &= -2\phi^3(\pi/2), \\ \phi'_R(-\pi/2) - \phi'_L(3\pi/2) &= -2\phi^3(-\pi/2), \end{aligned}$$

which leads to

$$\frac{2\alpha}{\pi}[A \sinh(\alpha) \pm B \cosh(\alpha)] = [A \cosh(\alpha) \pm B \sinh(\alpha)]^3. \quad (11)$$

A. Solutions

Possible solutions to Eqs. (11) are listed below (both A and B may be set to be real, for this purpose):

Asymmetric solution: For $A \neq 0$ and $B \neq 0$, we find the following nontrivial solution:

$$A_{as}^2 = \frac{\alpha}{\pi} \frac{\cosh(2\alpha) + 2}{\sinh(2\alpha)[\cosh(2\alpha) + 1]}, \quad (12)$$

$$B_{as}^2 = \frac{\alpha}{\pi} \frac{\cosh(2\alpha) - 2}{\sinh(2\alpha)[\cosh(2\alpha) - 1]}. \quad (13)$$

The non-negativity of B_{as}^2 requires that $\cosh(2\alpha) \geq 2$, hence the asymmetric solution exists at

$$\mu \leq -\frac{\ln(2 + \sqrt{3})^2}{2\pi^2} \approx -0.0879. \quad (14)$$

Obviously, there are two mutually symmetric representatives of the asymmetric solution (mirror images of each other).

Symmetric solution:

$$A_{sym}^2 = \frac{2\alpha}{\pi} \frac{\sinh(\alpha)}{(\cosh(\alpha))^3}, \quad B_{sym}^2 = 0, \quad (15)$$

Antisymmetric solution:

$$A_{anti}^2 = 0, \quad B_{anti}^2 = \frac{2\alpha}{\pi} \frac{\cosh(\alpha)}{(\sinh(\alpha))^3}. \quad (16)$$

Typical shapes of all three solutions are shown in Fig. 2. In both the symmetric and antisymmetric solutions, the two δ -functional nonlinear potentials trap equal populations; on the contrary, in the asymmetric solution one nonlinear potential traps a larger population than the other.

We also stress that for $\mu > 0$, the only possible solution is the anti-symmetric one in the case of self-attractive nonlinearity. From the Feynman's "no-node" theorem, it follows that for bosonic systems, such as those considered here, that the GS wave function has no nodes, hence the antisymmetric state cannot represent the GS. For this reason, below we concentrate on the symmetric and asymmetric solutions.

B. Characterizing symmetric and asymmetric solutions

With the expressions of A and B at hand, we can calculate other physical quantities of interest, such as the

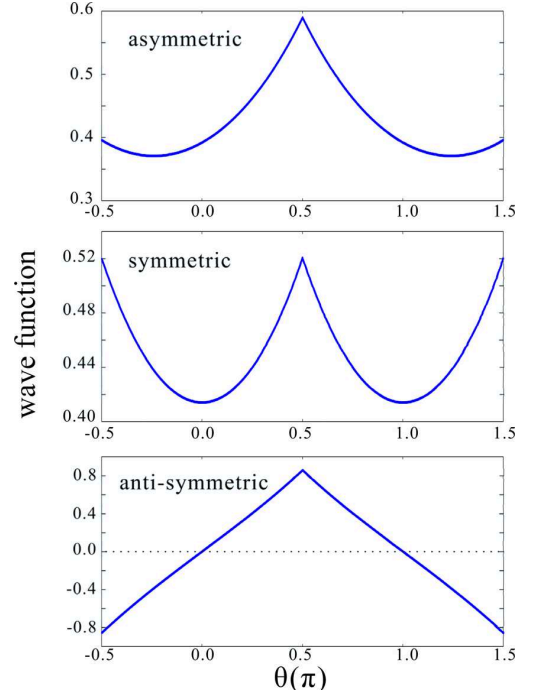


FIG. 2: (Color online) Examples of the different types of the solutions at $\mu = -0.1$.

energy and norm of the wave function. The total energy of the system can be written as

$$\begin{aligned} E &= \oint d\theta \left[-\phi \frac{1}{2} \frac{\partial^2}{\partial \theta^2} \phi - \frac{1}{2} U(\theta) |\phi(\theta)|^4 \right], \\ &= \mu N + \frac{1}{2} [|\phi|_{\theta \rightarrow \pi/2}^4 + |\phi|_{\theta \rightarrow -\pi/2}^4]. \end{aligned} \quad (17)$$

Thus, for the asymmetric and symmetric solutions, we obtain the following expressions for the norm and energy:

$$\begin{aligned} N_{as} &= 2 \int_{-\pi/2}^{\pi/2} \left[A_{as} \cosh(\sqrt{2|\mu|x}) + B_{as} \sinh(\sqrt{2|\mu|x}) \right]^2 \\ &= \frac{\cosh(2\alpha)^2 + 2\alpha \coth(2\alpha) - 2}{\sinh(2\alpha)^2}, \end{aligned} \quad (18)$$

$$E_{as} = -|\mu| [\operatorname{csch}(2\alpha)^2 + N - 1], \quad (19)$$

$$N_s = \frac{\sinh(\alpha)}{\cosh(\alpha)^3} (2\alpha + \sinh(2\alpha)), \quad (20)$$

$$E_s = \left(\frac{2\alpha}{\pi} \right)^2 \left[-\frac{N}{2} + \frac{\sinh(\alpha)^2}{\cosh(\alpha)^2} \right]. \quad (21)$$

The norm of the wave functions is shown in Fig. 3 as functions of the chemical potential. For the asymmetric state, N_{as} decreases monotonically as $|\mu|$ increases, approaching $N_{as} = 1$ at large $|\mu|$. In fact, in the limit of large $|\mu|$, or large $\alpha \equiv \sqrt{2|\mu|\pi/2}$, one has $\sinh(2\alpha) \approx \cosh(2\alpha) \approx e^{2\alpha}/2$, which simplifies the asymmetric solu-

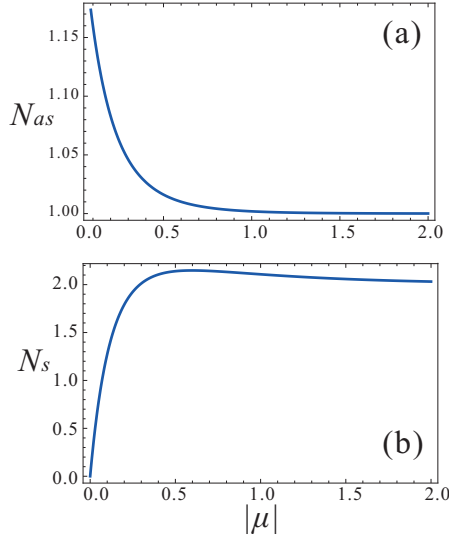


FIG. 3: (Color online) The norm of the asymmetric (a) and symmetric (b) states as functions of the chemical potential. The asymmetric state exists at $|\mu| > 0.0879$.

tion to the expressions whose norm is, indeed, $N_{as} = 1$:

$$\begin{aligned}\phi_L(\theta) &= (2|\mu|)^{1/4} e^{-\alpha} e^{\sqrt{2|\mu|}\theta}, \\ \phi_R(\theta) &= (2|\mu|)^{1/4} e^{-\alpha} e^{\sqrt{2|\mu|}(\theta-\pi)}.\end{aligned}$$

According to the Vakhitov-Kolokolov criterion [23], localized stationary modes in the system with the self-focusing nonlinearity are dynamically unstable if $dN/d\mu > 0$. We thus conclude, from Fig. 3, that the whole asymmetric branch, and the symmetric one at $|\mu| > 0.5$ are unstable, cf. a similar conclusion made for the infinite system in Ref. [13]. To confirm conclusion, we performed direct simulations of the time-dependent GP equation (4). The δ -functions were modeled by a very narrow Gaussian, as defined by Eq. (3) with $a = 0.02$. We took different analytic solutions as the initial wave function and followed its evolution. Figure 4 displays the results, from which we have indeed confirmed that only the symmetric solution at $|\mu| < 0.5$ is stable. In addition, for the asymmetric solution, exhibiting temporal oscillation between two degenerate unstable asymmetric states.

For a given norm $N_{as} = N_s \equiv N$, the GS can be identified by comparing the energies of the coexisting states. This is shown in Figs. 5(a) and (b), in which both the energies and chemical potentials are plotted versus the common norm of the asymmetric and symmetric states, in the range of $1.01 \leq N \leq 1.17356$, where the asymmetric solution exists. As seen from Fig. 5(a), the energies of both solutions decrease as the norm increases. However, the symmetric state always has the *lower energy*, hence it represents the GS for the given norm. This conclusion is consistent with the fact that the asymmetric state is always dynamically unstable, according to Fig. 4.

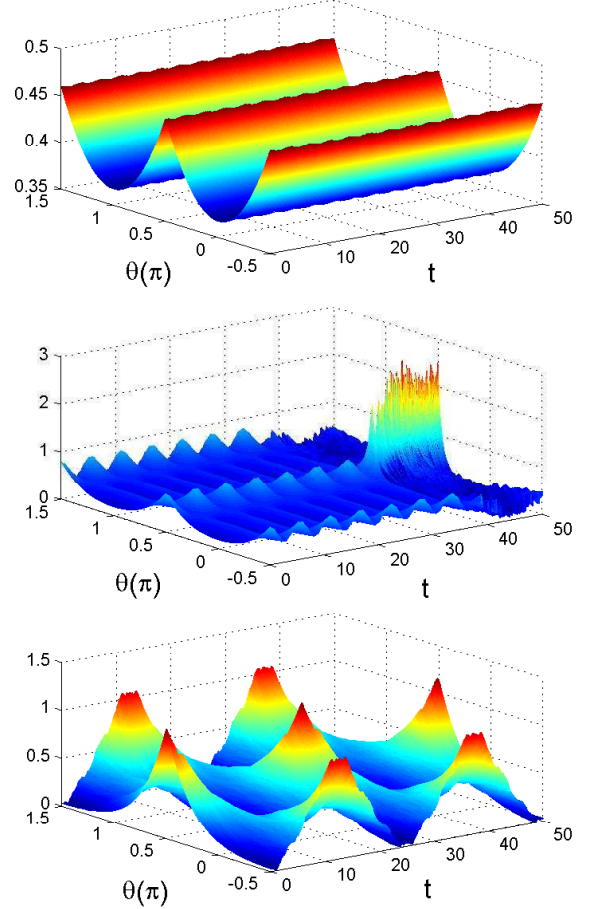


FIG. 4: (Color online) The time evolution of the wave function in direct simulations of the model with the delta-functions modeled by the narrow Gaussians. From top to bottom, the initial state is given by the symmetric solution at $|\mu| = 0.1$, the symmetric solution at $|\mu| = 1$, and the asymmetric one at $|\mu| = 1$. Only the top solution is stable.

Figure 5(b) demonstrates that the chemical potential of the symmetric state is weakly sensitive to the norm. As a consequence, the energy of the symmetric state decreases roughly linearly with N , which can be deduced from Eq. (21) and is seen in Fig. 5(a).

An important characteristic of the asymmetric state is the *population imbalance*, which is defined as

$$\Theta \equiv \frac{\int_0^{\pi/2} |\phi(\theta)|^2 d\theta - \int_{-\pi/2}^0 |\phi(\theta)|^2 d\theta}{\int_{-\pi/2}^{\pi/2} |\phi(\theta)|^2 d\theta}, \quad (22)$$

to quantify the asymmetry of the populations trapped by the two nonlinear potential wells. For the exact asymmetric solution obtained here, the population imbalance is

$$\Theta = \frac{\sinh(2\alpha)^2 \sqrt{\cosh(2\alpha)^2 - 4}}{[\cosh(2\alpha) + 1][\cosh(2\alpha)^2 + 2\alpha \coth(2\alpha) - 2]}. \quad (23)$$

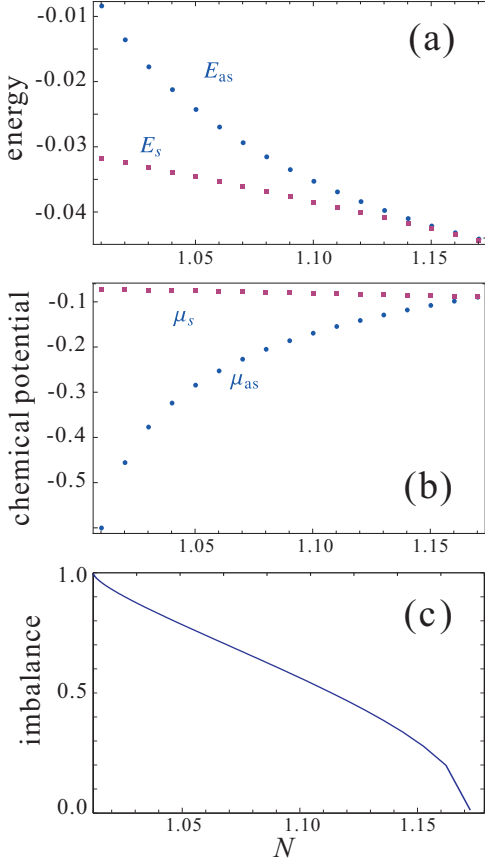


FIG. 5: (Color online) The energy (a) and chemical potential (b) of the symmetric and asymmetric states as functions of the norm. (c) Imbalance Θ for the asymmetric state as a function of the norm. All the quantities plotted have been rescaled to be dimensionless.

It is plotted in Fig. 5(c) as a function of the norm. As the norm increases from $N = 1$, Θ decreases monotonically from 1 until it vanishes at the critical norm, $N_c = 1.17356$, where the asymmetric solution merges with the symmetric one and ceases to exist.

IV. NUMERICAL RESULTS FOR THE GAUSSIAN-SHAPED NONLINEARITY

We now turn to the system with the ideal δ -functions replaced by the Gaussians with finite width, as shown in Eq. (3). To this end, we have to resort to numerical solutions of the GP equation (5). As in the case of δ -functions, the key issue is whether the GS is symmetric or asymmetric. Note that, for nonlinear potentials $U(\theta)$ with finite width a , the GS always exists with the norm $N \sim a^2|\mu|$ for $\mu \rightarrow -\infty$, in contrast to the analytical result for δ -functional nonlinearity, where the steady-state solution can be found only in a finite range of the values of N [22], cf. Fig. 3(b).

Numerically found characteristics of the system with

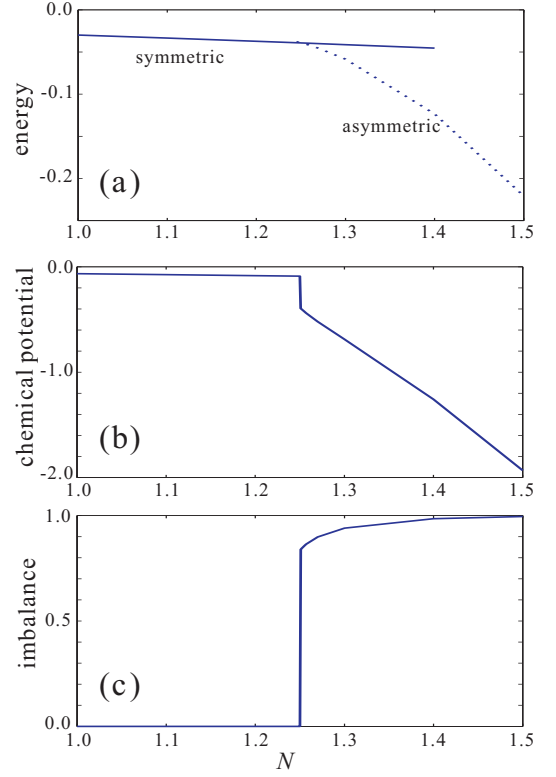


FIG. 6: (Color online) (a) Energies of the symmetric and asymmetric states as functions of the norm in the model with the Gaussians of width $a = 0.1$. (b) The chemical potential of the ground state. (c) The population imbalance of the ground state.

the Gaussian nonlinear potential, with width $a = 0.1$, are displayed in Fig. 6. In Fig. 6(a), we observe that, for $N < N_c = 1.25$, the GS is represented by the symmetric mode, whose energy decreases nearly linearly with N , in agreement with the results reported above for δ -functional model [cf. Fig. 5(a)]. However, at the critical value of the norm, $N_c = 1.25$, there emerges the asymmetric mode, whose energy is lower than in the symmetric one. Thus, the symmetry-breaking phase transition takes place at $N = N_c$, changing the GS from symmetric to asymmetric. As shown above, such a transition does not occur in the case of δ -functional nonlinear potential. Focusing on the GS properties, we plot its chemical potential and population imbalance in Fig. 6(b) and (c), respectively. At the critical point N_c , both these quantities exhibit a sudden jump, indicating that the phase transition at this point is of first kind (alias, it is a *subcritical bifurcation* of the stationary states).

The critical norm N_c increases with the width of the Gaussian, a , while both the jumps of the chemical potential and imbalance at N_c decrease, and eventually vanish at the respective critical value, $a_{\text{crit}} \simeq 0.28$. An example is presented in Fig. 7 for $a = 0.3$. Similar to the previous case, there is a symmetry-breaking phase transition at the critical value of the norm, which is now $N_c = 1.54$.

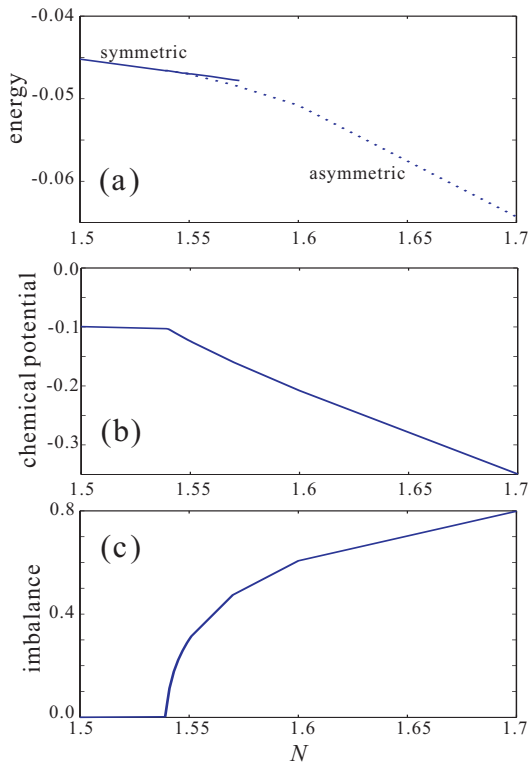


FIG. 7: (Color online) Same as Fig. 6, but for the width of the Gaussian $a = 0.3$.

However, differently from the case of $a = 0.1$, the transition here is of second kind (in other words, it is represented by a *supercritical bifurcation*), as can be seen in the plots of the GS chemical potential and imbalance, in Figs. 7(b) and (c), respectively — both quantities are continuous functions of N , although both exhibit kinks at $N = N_c$.

Figure 8 shows that the numerically found critical norm N_c increases almost linearly with the Gaussian's width a . As shown above, the system features the symmetry-breaking QPT of the first kind, with jumps of the population imbalance and chemical potential, at $a < a_{\text{crit}} \simeq 0.28$, see Fig. 9. Actually, the chemical-potential jump, $\Delta\mu$, increases almost exponentially as a decreases. On the other hand, at $a > a_{\text{crit}}$, the continuous QPT of the second kind occurs, without jumps. Thus, the type of the QPT from the symmetric state to the asymmetric one is sensitive to the width of nonlinear potential well. Plausibly, a similar mechanism determines the type of the symmetry-breaking QPT which happens in a the BEC trapped in the 1D nonlinear ring-shaped lattice, which was considered in Ref. [12].

V. DISCUSSION

Our analysis demonstrates that, even though the Gaussian nonlinear potential with width a , represented by

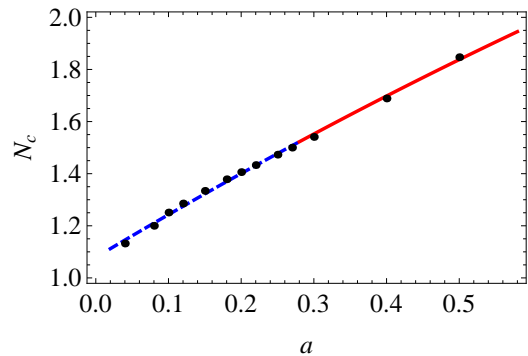


FIG. 8: (Color online) The numerically found critical norm, N_c , as a function of the width of the nonlinearity-modulation Gaussian, a . The symmetry-breaking phase transition of the first kind occurs at $a \leq a_{\text{crit}} \simeq 0.28$ (the dashed line), while the solid line indicates the phase transition of the second kind, which occurs at $a > a_{\text{crit}}$.

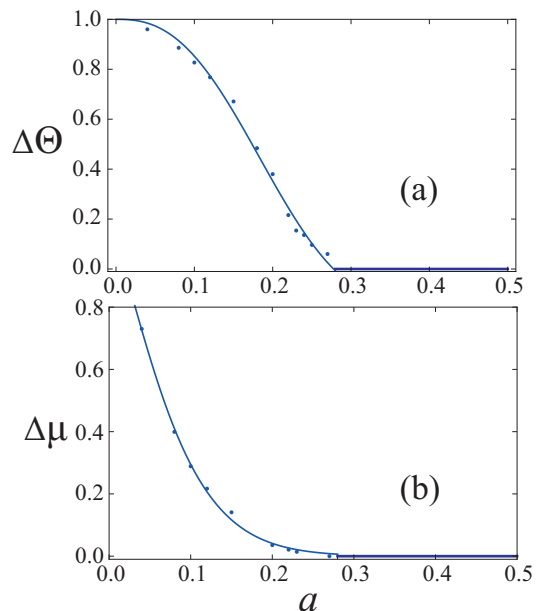


FIG. 9: (Color online) (a) The jump of the population imbalance $\Delta\Theta$ of the ground state at the critical point, $N = N_c$, as a function of width a . At $a \lesssim 0.28$, the order phase transition of the first kind occurs at $N = N_c$. (b) The jump of the chemical potential, $\Delta\mu = \mu_s - \mu_{\text{as}}$, between the symmetric and asymmetric states at the transition point, $N = N_c$ for different value of the Gaussian's width, a .

Eq. (3), reduces to the δ -functional potential (2) in the limit of $a \rightarrow 0$, there are several essential differences between them:

(1) The Gaussian potential always exhibits the symmetry-breaking phase transition, which changes the GS from symmetric to asymmetric, at the critical value of the norm. The transition is of first kind for small widths a , and of the second kind at larger a . Such a phase tran-

sition does not occur in the model with the δ -functional potential, the GS being always symmetric.

(2) In the case of the δ -functional potential, the asymmetric state exists only in the range of norms $N \in (1.0, 1.17356)$, and the corresponding population imbalance decreases from 1 to 0 as N increases from 1 to 1.17356. In the case of the Gaussian potential, the asymmetric state always exists at sufficiently large N , and the imbalance increases with the norm.

These observations indicate that the δ -functional nonlinear potential is degenerate: as soon as the potential is given a finite width, a length scale is introduced into the system, which changes its properties dramatically. Such singular behavior also occurs for a single nonlinear δ -functional potential with the cubic nonlinearity [24–26], as well as for the pair of δ -functions in the infinite system [13, 26]. In reality, one can never implement the ideal δ -functional profile. Intuitively, one may expect that the physics of the δ -potential may be recovered by real potentials in a proper limit. This is indeed the case for the linear δ -functional potential (also known as the Fermi potential), examples of which appear in textbooks on quantum mechanics. However, our analysis and that in Refs. [13] and [26] demonstrate that the physics of the nonlinear δ -potential is qualitatively different from its any counterpart of a finite width. On the other hand, the degenerate character of the nonlinear potential based on the ideal δ -function(s) may be lifted not only by lending it a finite width, but also by combining it with a periodic linear potential, which also introduces a particular length scale into the system [26].

VI. CONCLUSION

Within the framework of the mean-field theory, we have performed a systematic analysis of the BEC dynamics in the ring-shaped trap with nonlinear double-well potentials, represented by the pair of δ -functional or Gaussian modulation functions, placed at diametrically opposite points of the ring. Our studies show that, in the case of the Gaussian-type nonlinear double-well potential, the

GS (ground state) of bosons always undergoes the transition from symmetric to asymmetric states, as the norm of the condensate increases. The type of the transition is determined by the width of the Gaussian. There exists a critical value of the width, $a_{\text{crit}} \simeq 0.28$ (in terms of the azimuthal coordinate), such that, at $a < a_{\text{crit}}$, the symmetry-breaking phase transition is of the first kind (in other words, it is a subcritical bifurcation of the stationary states), while, at $a > a_{\text{crit}}$, the transition is of the second kind (associated with the supercritical bifurcation). This result, in particular, answers a question left open in Ref. [12], to explain how the type of the phase transition depends on the period of spatial modulation, which determines the length scale of the nonlinear potential. For the case of δ -functional nonlinear double-well potential, we have obtained the analytical solution of the time-independent GP equation. However, in that case the GS is always a symmetric state. The asymmetric state exists within a narrow range of values of the norm, being always dynamically unstable, and featuring the energy which is higher than in the coexisting symmetric state. These properties for the δ -functional nonlinear potential are qualitatively different from those of the Gaussian nonlinear potential well with any finite width.

Acknowledgments

This work was funded, in a part, by National Basic Research Program of China 2011CB921204, National Natural Science Foundation of China (Grant Nos. 60921091, 10874170, 11004186), CUSF, and Research Fund for the Doctoral Program of Higher Education of China (Grant No. 20103402110024, 20103402120031). Z. -W. Zhou gratefully acknowledges the support of the K. C. Wong Education Foundation, Hong Kong. H.P. is supported by the US NSF and the Welch Foundation (Grant No. C-1669). The work of B.A.M. is partly supported by grant No. 2010239 from the Binational (US-Israel) Science Foundation.

-
- [1] P. C. Hohenberg, Phys. Rev. 158, 383 (1967).
 - [2] V. Bagnato and D. Kleppner, Phys. Rev. A 44, 7439 (1991).
 - [3] K. E. Strecker, G.B. Partridge, A. G. Truscott, and R. G. Hulet, Nature (London) 417, 150 (2002).
 - [4] L. Khaykovich, F. Schreck, G. Ferrari, T. Bourdel, J. Cubizolles, L. D. Carr, Y. Castin, and C. Salomon, Science 296, 1290 (2002).
 - [5] S. L. Cornish, S. T. Thompson, and C. E. Wieman, Phys. Rev. Lett. 96, 170401 (2006).
 - [6] J. A. Sauer, M.D. Barrett, and M.S. Chapman, Phys. Rev. Lett. 87, 270401 (2001); S. Gupta, K. W. Murch, K. L. Moore, T. P. Purdy, and D. M. Stamper-Kurn, Phys. Rev. Lett. 95, 143201 (2005); A. S. Arnold, C. S. Garvie, and E. Riis, Phys. Rev. A 73, 041606 (2006); O. Morizot, Y. Colombe, V. Lorent, H. Perrin, and B. M. Garraway, Phys. Rev. A 74, 023617 (2006); A. Ramanathan, K. C. Wright, S. R. Muniz, M. Zelan, W. T. Hill, C. J. Lobb, K. Helmerson, W. D. Phillips, and G. K. Campbell, Phys. Rev. Lett. 106, 130401 (2011); B. E. Sherlock, M. Gildemeister, E. Owen, E. Nugent, and C. J. Foot, Phys. Rev. A 83, 043408 (2011).
 - [7] E. Tiesinga, B. J. Verhaar, and H. T. C. Stoof, Phys. Rev. A 47, 4114 (1993); E. Timmermans, P. Tommasini, M. Hussein, and A. Kerman, Phys. Rep. 315, 199 (1999).
 - [8] F.K. Fatemi, K.M. Jones, and P.D. Lett, Phys. Rev. Lett.

- 85**, 4462 (2000); M. Theis, G. Thalhammer, K. Winkler, M. Hellwig, G. Ruff, R. Grimm, and J. H. Denschlag, Phys. Rev. Lett. **93**, 123001 (2004); R. Yamazaki, S. Taie, S. Sugawa, and Y. Takahashi, Phys. Rev. Lett. **105**, 050405 (2010); S. Blatt, T. L. Nicholson, B. J. Bloom, J. R. Williams, J. W. Thomsen, P. S. Julienne, and J. Ye, Phys. Rev. Lett. **107**, 073202 (2011).
- [9] T. Killian, private communications.
- [10] For a recent view, see for example, C. Chin, R. Grimm, P. Julienne, and E. Tiesinga, Rev. Mod. Phys. **82**, 1225 (2010).
- [11] H. Sakaguchi and B. A. Malomed, Phys. Rev. E **72**, 046610 (2005); F. K. Abdullaev and J. Garnier, Phys. Rev. A **72**, 061605(R) (2005); G. Theocharis, P. Schmelcher, P. G. Kevrekidis, and D. J. Frantzeskakis, *ibid.* **72**, 033614 (2005); Y. Sivan, G. Fibich, and M. I. Weinstein, Phys. Rev. Lett. **97**, 193902 (2006); G. Fibich, Y. Sivan, and M. I. Weinstein, Physica D **217**, 31 (2006); H. Sakaguchi and B. A. Malomed, Phys. Rev. E **73**, 026601 (2006); J. Belmonte-Beitia, V. M. Perez-Garcia, V. Vekslerchik, and P. J. Torres, Phys. Rev. Lett. **98**, 064102 (2007); Y. Kominis and K. Hizanidis, Opt. Express **16**, 12124 (2008); Y. V. Kartashov, V. A. Vysloukh, and L. Torner, Opt. Lett. **33**, 1747 (2008); V. Perez-Garcia and R. Pardo, Physica D **238**, 1352 (2009); N. V. Hung, P. Ziń, M. Trippenbach, and B. A. Malomed, Phys. Rev. E **82**, 046602 (2010).
- [12] Z.-W. Zhou, S.-L. Zhang, X.-F. Zhou, G.-C. Guo, X. Zhou, and H. Pu, Phys. Rev. A **83**, 043626 (2011).
- [13] T. Mayteevarunyoo, B. A. Malomed, and G. Dong, Phys. Rev. A **78**, 053601 (2008).
- [14] Y. V. Kartashov, B. A. Malomed, and L. Torner, Rev. Mod. Phys. **83**, 247 (2011).
- [15] K. Winkler, G. Thalhammer, F. Lang, R. Grimm, J. H. Denschlag, A. J. Daley, A. Kantian, H. P. Büchler, and P. Zoller, Nature Physics **441**, 04918 (2006); R. Qi and H. Zhai, Phys. Rev. Lett. **106**, 163201 (2011).
- [16] L. D. Carr, C. W. Clark, and W. P. Reinhardt, Phys. Rev. A **62**, 063610 (2000).
- [17] L. D. Carr, C. W. Clark, and W. P. Reinhardt, Phys. Rev. A **62**, 063611 (2000).
- [18] R. Kanamoto, H. Saito, M. Ueda, Phys. Rev. A **67**, 013608 (2003).
- [19] A. Parola, L. Salasnich, R. Rota, and L. Reatto, Phys. Rev. A **72**, 063612 (2005); R. Kanamoto, H. Saito, and M. Ueda, *ibid.* **73**, 033611 (2006); L. Salasnich, A. Parola, and L. Reatto, *ibid.* **74**, 031603(R) (2006); M. Modugno, C. Tozzo, and F. Dalfovo, *ibid.* **74**, 061601(R) (2006); I. Lesanovsky and W. von Klitzing, Phys. Rev. Lett. **98**, 050401 (2007); A. V. Carpentier and H. Michinel, Europ. Lett. **78**, 10002 (2007); J. Brand, T. J. Haigh, and U. Zülicke, Phys. Rev. A **80**, 011602(R) (2009); J. Smyrnakis, S. Bargi, G. M. Kavoulakis, M. Magiropoulos, K. Kärkkäinen, and S. M. Reimann, Phys. Rev. Lett. **103**, 100404 (2009); J. Smyrnakis, M. Magiropoulos, G. M. Kavoulakis, and A. D. Jackson, Phys. Rev. A **81**, 063601 (2010); M. Abad, M. Guilleumas, R. Mayo, M. Pi, and D. M. Jezek, Europ. Lett. **94**, 10004 (2011).
- [20] L. C. Qian, M. L. Wall, S. Zhang, Z. Zhou, and H. Pu, Phys. Rev. A **77**, 013611 (2008).
- [21] M. Abad, M. Guilleumas, R. Mayol, M. Pi, and D.M. Jezek, Phys. Rev. A **81**, 043619 (2010); S. Zöllner, G. M. Bruun, C. J. Pethick, and S. M. Reimann, Phys. Rev. Lett. **107**, 035301 (2011).
- [22] V. A. Brazhnyi and B. A. Malomed, Phys. Rev. A **83**, 053844 (2011).
- [23] M. Vakhitov and A. Kolokolov, Radiophys. Quantum Electron. **16**, 783 (1973).
- [24] B. A. Malomed and M. Ya. Azbel, Phys. Rev. B **47**, 10402 (1993).
- [25] M. I. Molina and C. A. Bustamante, Am. J. Phys. **70**, 67 (2002).
- [26] N. Dror and B. A. Malomed, Phys. Rev. A **83**, 033828 (2011).